Spectroscopic characterization and photo catalytic degradation ability of ternary oxides of Cobalt

Moushumi Dutta Purkayastha[1], Partha Pratim Ray[2], Tapas Pal Majumder[1], Mitali Sarkar[3]*

[1]Department of Physics, University of Kalyani-741235, West Bengal, India
[2]Department of Physics, Jadavpur University, Kolkata-700032, West Bengal, India
[3]Department of Chemistry, University of Kalyani, Kalyani-741235, West Bengal, India

Email: borahmou@gmail.com

Abstract

In the present work we have prepared and characterized the two ternary forms of cobalt titanate namely ilmenite and cubic by the sol-gel technique simply by replacing the titanium precursor and using a cationic surfactant micelle solution followed by calcinations at 600°C and 800°C respectively. In both cases, the nanopowders revealed a dark bluish green color, different morphologies of spherical, rhombus and needle shapes with mean particle sizes 29 and 37 nm, respectively. Bearing growing environmental concerns in mind, we have also highlighted a simple nano chemistry based clean and efficient process for effective degradation of hazardous malachite green oxalate dye by an in-situ ultraviolet irradiation set-up. In this field there is hardly any report involving comparative study of ternary oxides of cobalt as potential candidates for photo catalytic degradation. We ultimately observed that cobalt meta titanate proved itself the optimal catalyst at a calcination temperature of 600°C showing a maximum degradation efficiency of 96.38% It also showed a better first-order rate constant of 0.01636 min^{-1}. A decent attempt to correlate photoluminescence and photo catalysis has also been made. Also, a heterojunction has been fabricated with cobalt meta titanate and the parameters of crucial importance in photocatalysis namely conductivity, carrier mobility, transit time evaluated from the current-voltage characteristics.

Keywords: *Nanoparticles; CTAB micelle solution; Photocatalytic degradation; Reaction kinetics, Heterojunction*

1. Introduction

Dyes play a vital role in various branches of the dyeing and textile industries. Due to their high visibility, they are in fact the first contaminant to be recognized in industrial wastewater even in minute concentrations (<1 ppm) [1]. These colored wastewaters act as a considerable source of eutrophication as well as non-aesthetic pollution that can produce dangerous by-products by further oxidation, hydrolysis or other chemical reactions [2-5]. Konstantinou and Albanis [6] reported that industrial dye stuffs and textile dyes constitute one of the largest groups of toxic organic compounds. Apart from toxic effects [7], presence of dyes in water systems can reduce light penetration thereby resulting in decreased photosynthetic activity. They can even hamper biodegradation of microorganisms in water [8]. Therefore, the impact of dyes released into the environment has been studied extensively in last few years [9, 10].Advanced oxidation processes (AOPs) employing semiconducting particles can serve an efficient cure

in reducing the hazards of dye pollution [3]. In the last two decades, investigations related to composites of TiO_2 with transition metal oxides have attracted a great interest in view of their technological and fundamental scientific importance. The present study outlines the synthesis of ternary cobalt titanate oxides and checks their potential in degrading organic dye pollutants. The dye selected for study, MG, is a water soluble cationic dye that appears as a green crystalline powder and belongs to triphenylmethane category [11]. Proper treatment of effluents containing MG dye is particularly essential to decrease its impact on human and marine health [11]. An insight into the carrier transport properties has been provided for cobalt metatitanate by fabricating a Schottky diode. The space charge limited current (SCLC) theory was put forward to explain the photocurrent responses.

2. Results and discussion

2.1 Materials and method

The following materials were used as received commercially without further purification: TiO_2 anatase nanopowder, titanium (IV) n-butoxide, cobalt acetate tetra hydrate were purchased from Sigma Aldrich; stearic acid, CTAB from Loba Chemie and sodium hydroxide pellets (NaOH), malachite green oxalate dye from Merck.

In cobalt ortho titanate (Co_2TiO_4) synthesis; 0.01 moles (approx. 2.49 g) of cobalt acetate tetra hydrate was dissolved in 30ml distilled de ionized water. After stirring for about 30 minutes, an aqueous solution of NaOH prepared by dissolving 0.02 moles (approx. 0.799 g) of NaOH pellets in 10ml distilled de-ionized water was added drop wise which reacts to produce precipitation of Co $(OH)_2$. Then 0.01 moles of TiO_2 anatase powder was added to the above solution. An aqueous micelle solution of CTAB (0.01 moles CTAB in 30 ml distilled de-ionized water) was also added to the mixed solution under magnetic stirring at 100ºC. The reaction was continued till the volume of the slurry decreased appreciably. The colour of the residue was greyish at this stage. The as-synthesized slurry was then dried in an oven at 120^{o}C for 24 hours, ground to fine powder and calcined in air at 800 ºC which yielded Co_2TiO_4 nano powder.

In cobalt meta titanate ($CoTiO_3$) synthesis; 0.08 moles (approx. 22.758 g) of stearic acid was melted in a beaker at a temperature of 120 ºC. This took about 30 minutes. Then 0.02 moles (approx. 4.98 g) of cobalt acetate tetra hydrate was added to the melted stearic acid under magnetic stirring at the rate of 500 revolutions per second. The two components dissolved to form a purple color homogeneous solution at 120 °C after duration of 2 hrs. Next stoichiometric tetra butyl titanate (0.02 moles or approx. 6.82 ml) was added drop wise to the above solution till a reddish brown solution was obtained. This resultant solution was allowed to cool down to room temperature naturally, after which it was seen to partly crystallize. It was then dried in an oven at 120 °C for a period of 24 hours. The $CoTiO_3$ nano powder obtained was ground finely and then calcined at 600 °C for a period of 2 hours. Both the samples revealed a bluish green hue. The possible reaction pathways of both the ternary oxides of cobalt have been shown in figure 1(a) _1(b).

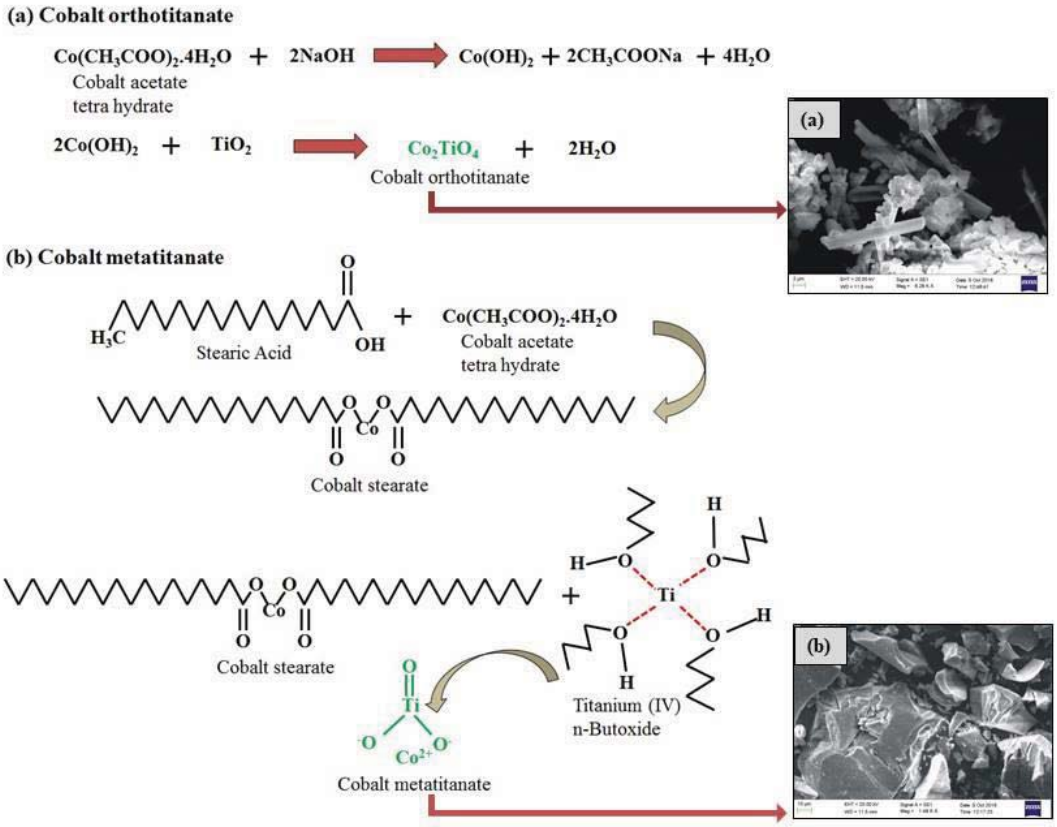

FIG 1.Reaction pathway of cobalt titanium oxide phases with focus laid on the main products (a) Co_2TiO_4 with corresponding SEM images at 1 µm magnification 6.28 K X and (b) $CoTiO_3$ with corresponding SEM images at 10 µm magnification 1.48 K X.

2.2. XRD analysis

An X-ray diffractometer (X'Pert PRO PANalytical) was operated at an accelerating voltage 30 kV and applied current 20 mA to characterize the products. The chemical identity of the products was determined by comparing the patterns to JCPDS standards. Figure 2 shows the peaks of Co_2TiO_4 well coinciding with JCPDS 39-1410. Some other peaks of TiO_2 anatase (JCPDS 84-1286), $CoTiO_3$ (JCPDS 77-1373), CoOOH (JCPDS 14-0673) and Co_3O_4 (JCPDS 76-1802) were also observed. The presence of cobalt oxide and hydroxides could be due to the oxidation of some Co^{2+} to Co^{3+} ions in the presence of surfactant CTAB [12- 14]. The calculated value of the mean particle size of Co_2TiO_4 was found to be 37 nm applying Scherer equation [15].

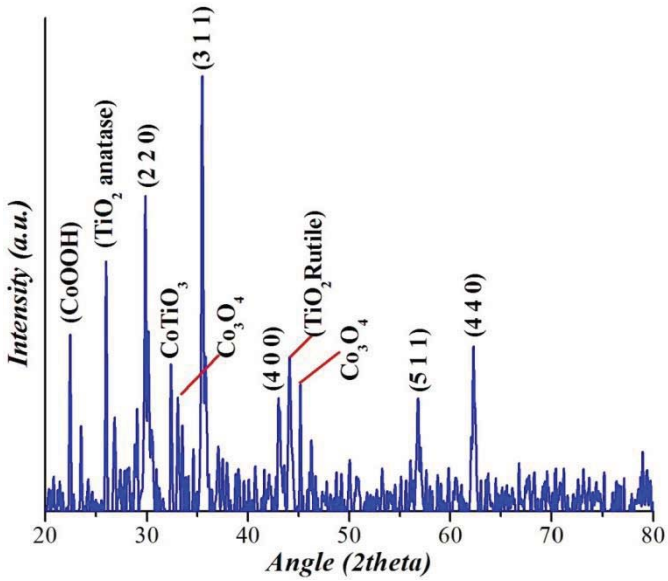

FIG 2. XRD of cubic Co_2TiO_4 calcined at 800 °C.

Ilmenite $CoTiO_3$ was formed at a temperature of 600 °C as illustrated in 'figure 3' coinciding well with the rhombohedral phase results indicated in JCPDS 77-1373. The mean particle size of the $CoTiO_3$ was found to be 29.8 nm. The use of stearic acid or the lower calcination temperature could have resulted in this phase which is in accordance with other reports [16-18].

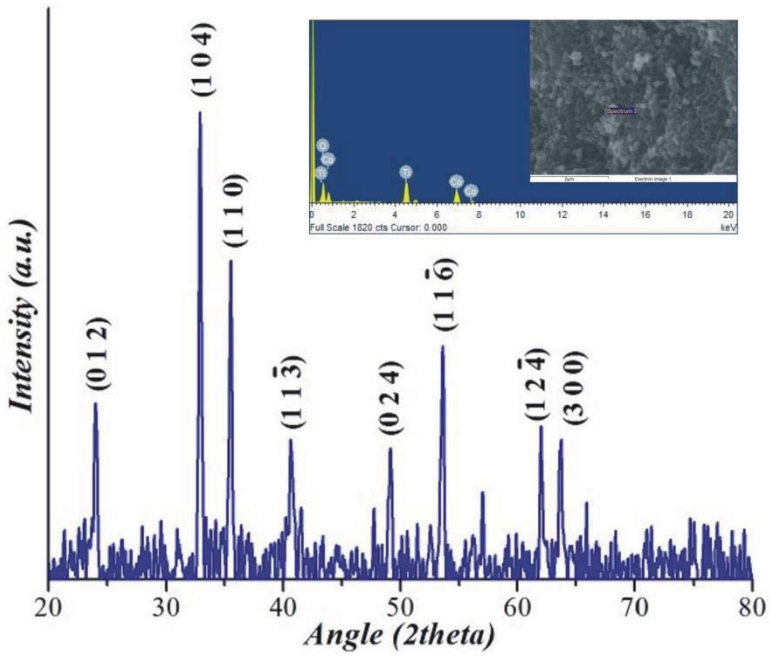

FIG 3. XRD of rhombohedral $CoTiO_3$ calcined at 600 °C inset EDS image of $CoTiO_3$.

2.3. SEM & EDS

Energy dispersive spectra (EDS) confirms the existence of cobalt and titanium metals in $CoTiO_3$ [inset figure 3]. Furthermore, neither N nor C signals signifying impurity were detected in the EDS spectrum. The morphology of the samples was ascertained by Scanning Electron Micrograph (SEM) Evo LS10, Zeiss. The SEM image for $CoTiO_3$ [figure 1(b)] demonstrates agglomerated irregular dark cloudy spherical shaped nanoparticles with spherical shape distributed all over the sample. The SEM images of Co_2TiO_4 reflect heterogeneous morphology [figure 1(a)]. Small rhombohedral structures arranged to form flower like and rod like structures.

2.4. UV-vis spectra results

Practical applications of nanoparticles are judged by their optical properties. UV-vis absorption spectra of both the samples were obtained with a UV 3600 spectrophotometer in the region 200 - 800 nm. Both Co_2TiO_4 and $CoTiO_3$ absorb light in the ultraviolet region ($\lambda < 370$ nm) which can be attributed to the (O^{2-}) → (Ti^{4+}) charge transfer [19]. The band gap of the two samples can be estimated by Tauc's plot. Both the samples are direct band gap semiconductors with $n = 1$. Graphs of $(\alpha h\nu)^{(2/n)}$ vs $h\nu$ are plotted where α and $h\nu$ stand for the absorbance and photon energy, respectively [20, 21]. The $h\nu$ value at the intersection point of the extrapolated linear portion of the curve and the horizontal axis specifies the value of the band gap. The UV-Vis absorbance versus wavelength spectra of $CoTiO_3$ shown in 'figure 4' well coincides with literature [22-24]. $CoTiO_3$ sample absorbs visible light in the wavelength range of 500 - 690 nm. It can thus be proposed that the absorbance in visible light region is mainly caused by $CoTiO_3$ because TiO_2 hardly absorbs visible light. There exist a small absorbance peak at 535 nm and a big one at 603.5 nm which is almost in close agreement with others [25]. The two absorbance peaks are defined by the ilmenite crystal structure of $CoTiO_3$. The Tauc's plot in the inset of 'figure 4' shows that the synthesized $CoTiO_3$ has a band gap of 2.53 eV, which originates from the $Co^{2+} \rightarrow Ti^{4+}$ charge-transfer transition. The UV-vis curve of Co_2TiO_4 as in 'figure 5' shows humps at around 520 and 615 nm in the visible region which are consistent with other results [26]. Tauc's plot in the inset of 'figure 5' indicates that the value of its direct band gap (E_g) is about 1.3 eV. The band gap value suggests that Co_2TiO_4 nanomaterial is a semi-conductor. Also, this value of band gap is in the same range as that of highly efficient photovoltaic cells. These results well highlight the ternary oxides of cobalt as promising candidates for photovoltaic cells as well.

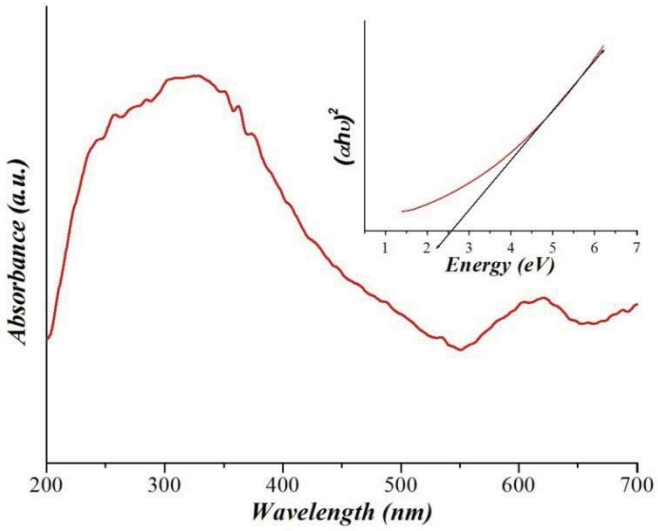

FIG 4. UV-visible spectra of $CoTiO_3$ calcined at 600 °C inset Tauc's plot of calcined $CoTiO_3$.

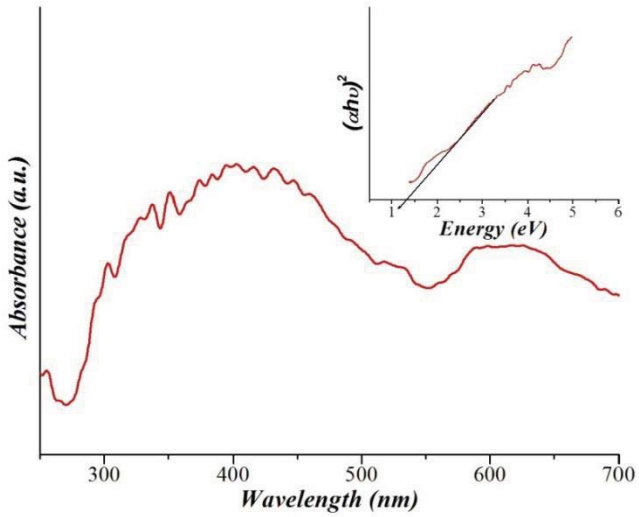

FIG 5. UV-visible spectra of Co_2TiO_4 calcined at 800 °C inset Tauc's plot of calcined Co_2TiO_4.

2.5. FT-IR results

FT-IR spectra of materials prepared in this study were recorded with a FT-IR spectrophotometer Perkin Elmer model name Spectrum one and model number L120-000A and are illustrated in 'figure 6' and 'figure 7' respectively. Infrared spectroscopy can however not distinguish between the two phase of cobalt titanate as the local coordination of the metal centres in them are similar. The presence of water on the powder surface can be assumed from the presence of the strong broad band centering at 1606 and 1639 cm^{-1} which is a signature of the δ (H-O-H) deformation vibration [27]. The broad bands at around 3408 and 3417 cm^{-1} are due to stretching vibrations of -OH groups [27]. The band at 2921 cm^{-1} is due to

the C-H stretching frequency. The band at 1367 cm^{-1} is accredited to COO- vibrations while that at 1374 cm^{-1} may be due to C-H bending frequency. The bands at 1081 and 1044 cm^{-1} are due to the -OBu groups (Bu = Butoxide) linked to Ti. The weak bands between 400 and 1000 cm^{-1} are due to the vibrations of Ti ions [26]. The Co-O-Ti stretching frequencies are observed at wave numbers of 762, 727 and 673 cm^{-1} [28-33]. Finally, the bands at 489, 480 cm^{-1} are credited to the Co-O and Ti-O stretching frequencies [26]. Consequently; these results support the formation of Co_2TiO_4, $CoTiO_3$ phases.

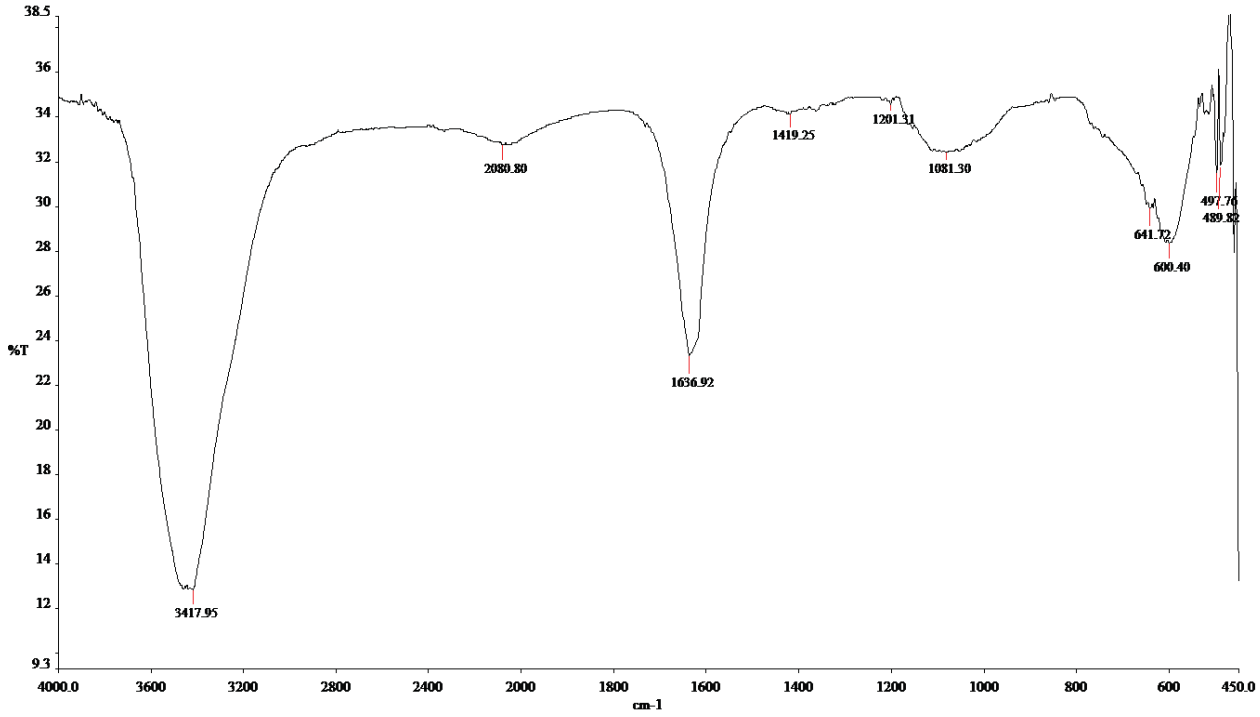

FIG 6. FT-IR spectra of $CoTiO_3$ calcined at 600 °C.

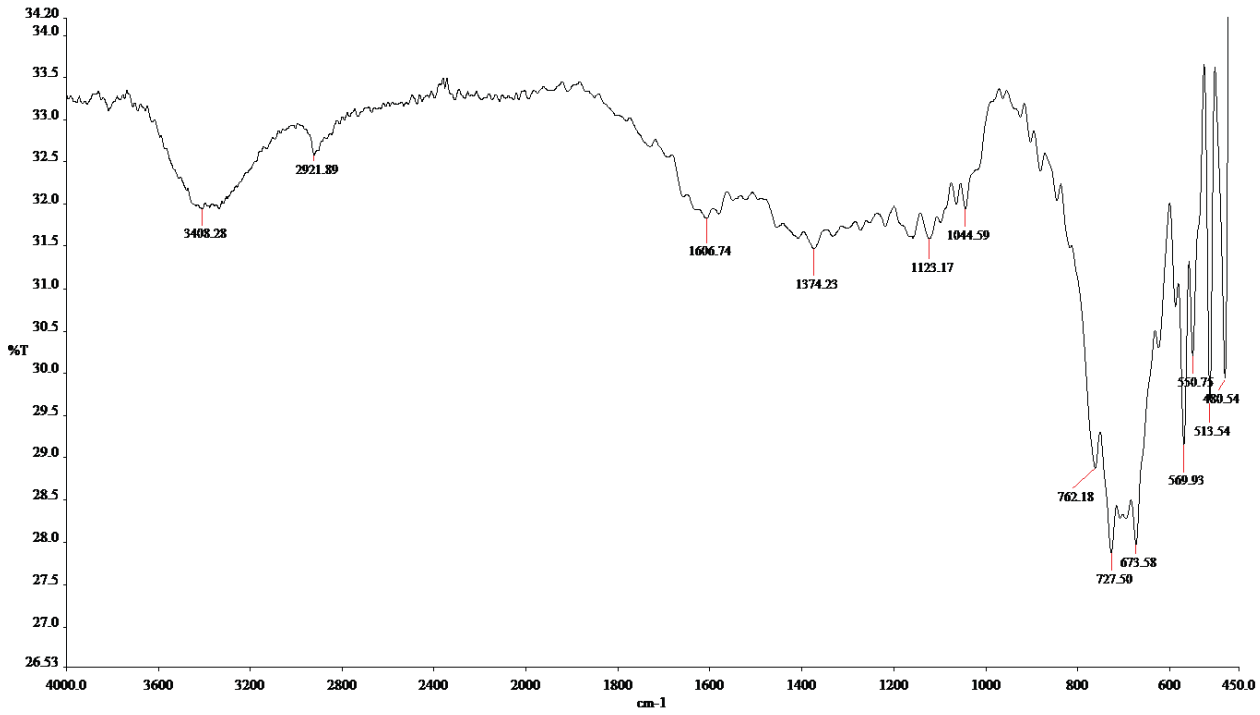

FIG 7. FT-IR spectra of Co_2TiO_4 calcined at 800 °C.

2.6. PL measurements

Photoluminescence (PL) measurements were recorded to elucidate the charge carrier recombination behaviour **using a** PTI QM 40 spectrophotometer. The intensity of PL signal provides a direct, qualitative measurement of the recombination rate of charge carriers [34]. Lower peak intensity indicate trapping and efficient separation of photogenerated carriers while high peak intensities indicate occurrence of rapid charge recombination [35-38]. In the present case, it is clearly seen that the PL intensity of the peaks of $CoTiO_3$ nanomaterial dispersed in chloroform and obtained by employing an excitation wavelength of 300 nm is lower than that of Co_2TiO_4 and TiO_2 [inset figure 8]. The emission peak of $CoTiO_3$ 'figure 8' was both narrow and sharp predicting bound excitation emission [39]. Lower peak intensity in case of $CoTiO_3$ means that the carriers generated are efficiently separated which is desirable for photocatalysis.

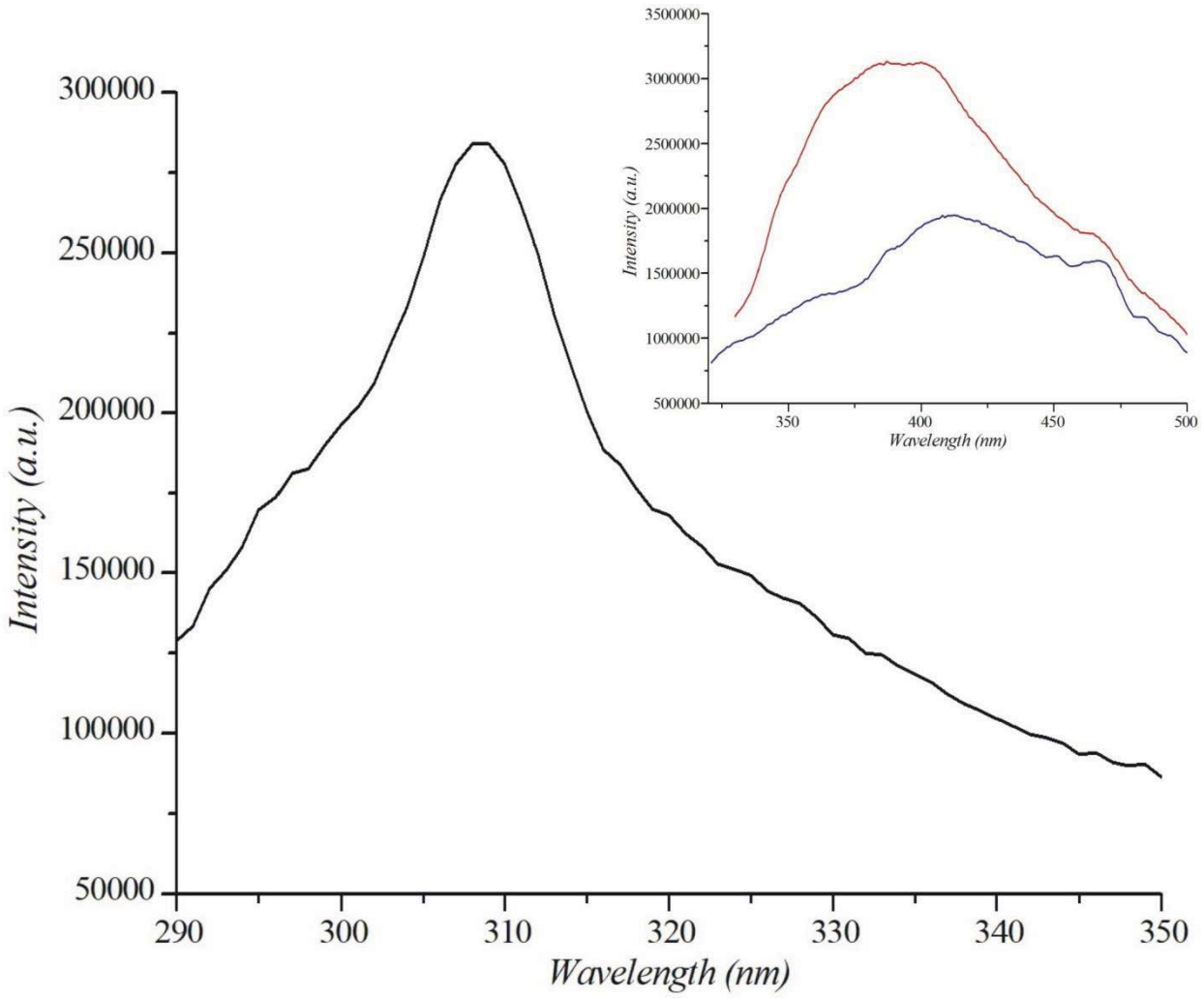

FIG 8. PL spectra of $CoTiO_3$ optimal catalyst in black (inset figure Co_2TiO_4 in red and TiO_2 in blue).

2.7. Photo degradation results

2.7.1. Effect of UV light intensity.

To investigate the effect of light intensity on the photo catalytic degradation of malachite green, different combinations of UV lamps were tested. The results as in 'figure 9(a)' indicate that degradation was accelerated as the intensity of light was increased, since any increase in the light intensity will increase the number of photons striking per unit area of semiconductor surface per unit time. However, the increase in degradation was not proportional to the increase in light intensity. This could be due to the fact that not all incident light gets absorbed. It depends on the free sites available on the surface of the catalyst. Further irradiation experiments were carried out with all the four UV lamps in ON condition.

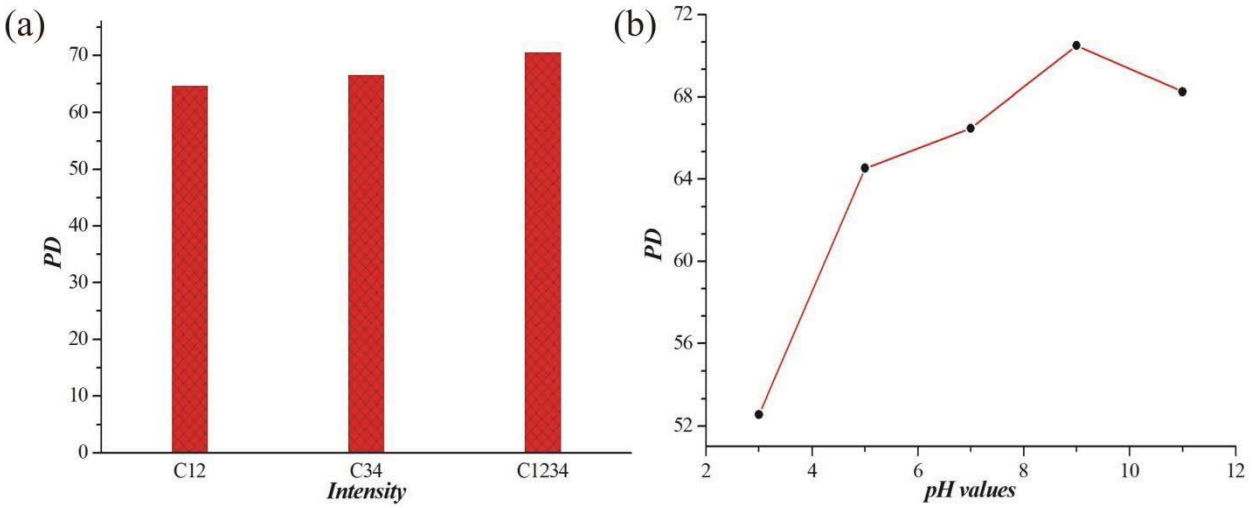

FIG 9. (a) Light intensity versus PD graph and (b) pH versus PD graph.

2.7.2. Effect of pH

Dye reaction rates are influenced in a number of ways by the pH of the solution. It can influence dye adsorption [40] as well as surface dependent properties [41]. Malachite Green is a cationic dye [11] and its degradation is favored at higher pH values on cobalt modified TiO_2. At pH values higher than pH_{pzc}, the surface of the catalyst gets negatively charged and vice versa [42, 43].Experiments were carried out and the optimal pH range was found to be 9-10 'figure 9(b)'.

2.7.3. Photocatalysis mechanism and reaction kinetics

When a photocatalyst is irradiated, electrons and holes are generated which give rise to free radicals. These active radicals can result in complete mineralisation of the dye pollutants [44, 45]. The photo catalytic degradation efficiency of the organic dyes was calculated using (1) [46].

$$PD = \frac{(A_o - A_t)}{A_o} \times 100 \quad (1)$$

Where A_o and A_t are the dye concentrations before and after irradiation.

The data of percentage degradation efficiency and rate constant are summarised in 'Table 1'

Table 1: Degradation data of MG dye using Co-Ti-O photo catalysts.

Sample type	Time (min)	Degradation efficiency (%)	Rate constant (k_1) (min^{-1})	Reused rate constant (min^{-1})
$CoTiO_3$	180	96.38	0.01636	0.01386
Co_2TiO_4	200	88.05	0.00983	0.00894

The absorbance of MG solution after exposure to UV light and cobalt titanate phases showed a sharp decline after 60 min indicating that they have good degrading capability. It was expected that Co_2TiO_4 reflecting heterogeneous morphology would show better degrading capability but considering both photo catalytic activity and cost effectiveness; $CoTiO_3$ synthesized at a calcination temperature of 600°C was chosen as the optimal photo catalyst. This could possibly be due to the higher surface area of $CoTiO_3$ which might have rendered larger number of active sites. Figure 10(a) compares photo catalytic degradation kinetics of MG dye by $CoTiO_3$ with Co_2TiO_4 respectively. Cobalt metatitanate showed the best photo degradation ability up to 96.38%.

The first-order kinetic model was tested to understand the order of photo catalytic degradation reaction [47, 48]:

$$\ln\left(\frac{A_o}{A_t}\right) = k_1 t \tag{2}$$

Where A_o and A_t denote initial and final MG concentrations (mg/L). It was observed that the first-order model could adequately interpret the kinetic data (R ~ 0.98), with much better fittings [Figure 10 (b)].

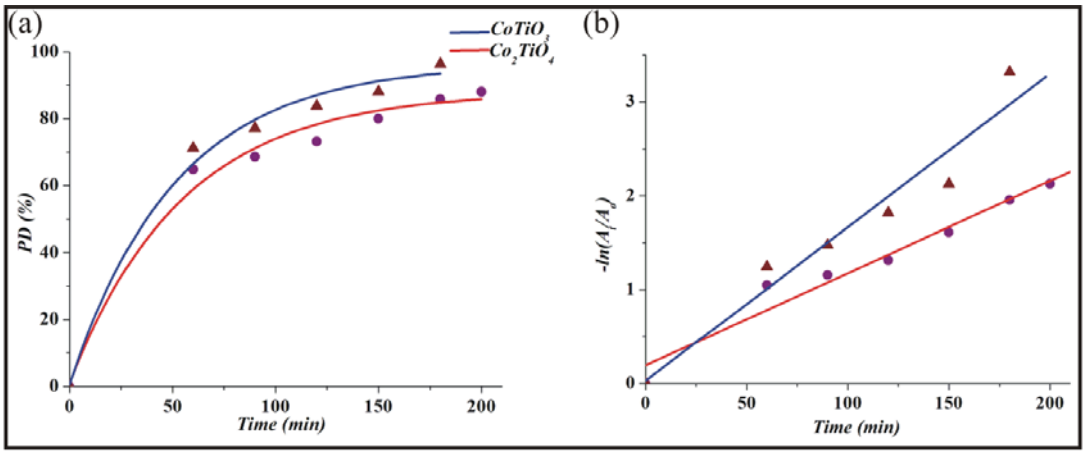

FIG 10. Degradation kinetics (a) PD versus time (b) –ln (A_t/A_o) versus time of $CoTiO_3$ indicated by triangle and Co_2TiO_4 indicated by circle.

Figure 11(a) draws a comparison between the rate constant values (k_1) for MG degradation by different cobalt titanate phases. The decrease in degradation rate of MG dye in case of cobalt ortho titanate can be attributed to bigger particle size that results after calcination. Due to evaporation of surfactant molecules oxygen content on the surface decreases and this can hamper photoactivity. Also, probably the surface area of Co_2TiO_4 is lower than that of $CoTiO_3$. Guo et al. [49] also obtained matching trend of photo catalytic degradation of methyl orange using silica-titania. Finally, in order to evaluate the potential reusability of the materials, experiments were repeated using the same catalysts retrieved after subsequent filtering and drying. It was observed that the calcined samples retained their photo catalytic activity which clearly indicates their recyclability shown in the 'figure 11(b)'and data tabulated in 'Table 1'

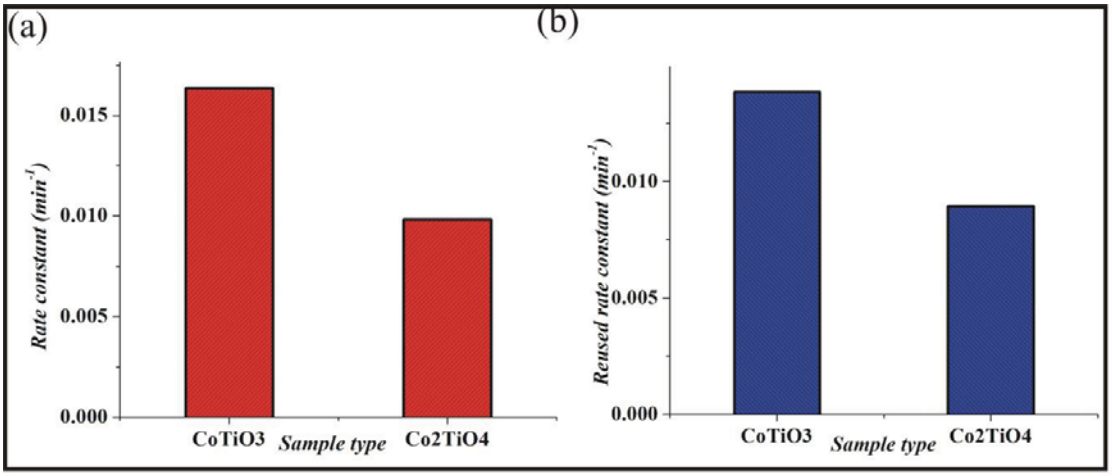

FIG 11. (a) Rate constant bar diagram for the two photo catalysts and (b) Bar diagram showing reusability of the samples.

2.8. Current-voltage (I-V) characteristics

The Indium tin oxide (ITO) substrate was cleaned in an ultrasonic bath and a dispersed solution of $CoTiO_3$ was spin coated (SCU 2700 spin coating unit) onto it to fabricate the ITO/$CoTiO_3$/Al diode. The film was then dried and its thickness (d) measured to be 1 μm with a surface profiler. To prepare the metal-semiconductor interface, aluminium metal was deposited on the fabricated film using a vacuum coating unit. The diode area (A) was estimated as 7.065×10^{-6} m^2.

I-V measurements were recorded under dark and illumination conditions by applying a bias voltage varying from -1V to +1V to the ITO/$CoTiO_3$/Al Schottky device and plotted in Figure 12(a). The calculated values of σ_{dark} and σ_{light} were 3.52×10^{-8} and 1.01×10^{-7} Sm^{-1}. The I-V graphs were further analysed using space charge limited conduction (SCLC) theory. lnI-lnV graphs were plotted under dark and illumination conditions [Figure 12(b)]. The graphs could be distinctly divided into two regions. The first region obeyed Ohm's law while the second region was governed by the SCLC transport mechanism. $I\text{-}V^2$ graphs were plotted [Figure 12(c)] taking the second region into consideration. The effective carrier mobility (μ_{eff}) was calculated using Mott-Garney equation (3) [50]

$$I = \frac{9\mu_{eff}\varepsilon_o\varepsilon_r A}{8}\left(\frac{V^2}{d^3}\right) \quad (3)$$

Where ε_0 and ε_r denote the dielectric permittivity in vacuum and the dielectric constant of the semiconductor [51, 52]. The estimated values of μ_{eff} were 2.01×10^{-11} and 5.35×10^{-11} $m^2V^{-1}s^{-1}$ under dark and light conditions.

The distance taken by the carrier to travel from anode to cathode is the transit time (τ) and is also calculated from the second region of I-V characteristics using equation (4) [50].

$$\tau = \frac{9\varepsilon_o\varepsilon_r A}{8d}\left(\frac{V}{I}\right) \quad (4)$$

The values were 9.84×10^{-6} and 2.08×10^{-5} s under light and dark conditions respectively. The lower transit time under illumination signifies light induced conduction mechanism.

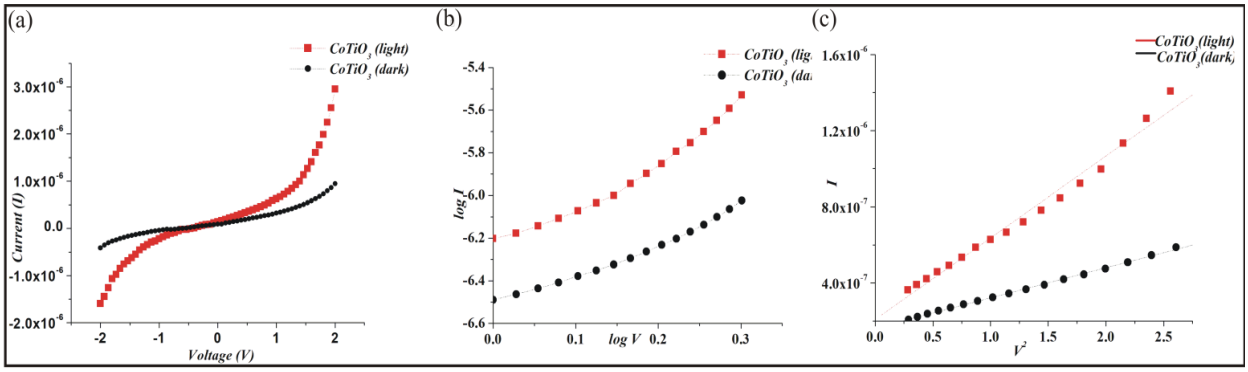

FIG 12. (a) Current-voltage characteristics of the ITO/$CoTiO_3$/Al Schottky device (b) ln I versus ln V plot to explain the conduction mechanism (c) I-V^2 plot to determine carrier mobility

Though the carrier transport properties did not appear to be appreciably enhanced in comparison to previous works [50] still the PCD abilities of the photocatalysts were good. This could have resulted from the high surface areas of the catalysts.

3. Conclusion

This study developed and tested the two ternary oxides of cobalt for enhanced photo catalytic degradation of malachite green oxalate dye under UV light. $CoTiO_3$ exhibited higher photo catalytic activity for degradation of MG dye under UV light, with a 96.38% removal rate in 3 hours. The first-order kinetic model could adequately interpret the kinetic data, and the apparent rate constant was determined to be 0.01636 min^{-1}which is higher than that of Co_2TiO_4.The cobalt meta titanate when employed as a Schottky diode possessed a mobility of 5.35×10^{-11} $m^2V^{-1}s^{-1}$ and a transit time of 9.84×10^{-6} s under illumination. Thus, cobalt titanates can effectively serve as electron transfer mediators inhibiting recombination of the

electron-hole pairs. This study predicts optoelectronic applicability and the use of heterojunction in degrading organic pollutants.

4. Acknowledgements

Authors appreciate the DST-PURSE program and CIL center, University of Kalyani for providing instrumental facilities. First author (M.D.P) thanks Dr. Yatramohan Jana for providing furnace facility, Dr. J.S Roy and research scholar Debalina Deb for instrumental handling assistance.

REFERENCES

[1] C. Kulsi, A. Ghosh, A. Mondol, K. Kargupta, S. Ganguly, D. Banerjee S0169-4332 (16) 31932-8 doi.org/10.1016/j.apsusc.2016.09.063 (2015)

[2] A.K. Srivastava, Praveen M. Arora, S.K. Gupta, B.R. Chakraborty, S. Chandra, S. Toyoda, H. Bahadur J Mater Sci Technol 26 986-990 (2010).

[3] A. Ajmal, I. Majeed, R.N. Malik, H. Idriss, M.A. Nadeem RSC. Adv. 4 37003-37026 (2014).

[4] H. Zollinger Wiley-VCH (2003).

[5] R. Kant Nat. Sci. 04 22–26 (2012).

[6] I. K. Konstantinou, T.A. Albanis Appl. Catal. B 49 1–14 (2004).

[7] R. Nilsson, R. Nordlinder, U. Wass, B. Meding, L. Belin Br. J. Ind. Med. 50 65–70 (1993).

[8] A.G. Prado, L.B. Bolzon, C.P. Pedroso, A.O. Moura, L.L. Costa Appl. Catal., B 82 219–224 (2008).

[9] W. Walthall, J. Stark Environ. Pollut. 104 207–215 (1999).

[10] S. Tsuda, M. Murakami, N. Matsusaka, K. Kano, K. Taniguchi, Y.F. Sasaki Toxicol. Sci. 61 92–99 (2001).

[11] N.P. Raval, P.U. Shah, N.K. Shah Appl Water Sci doi: 10.1007/s13201-016-0512-2 (2016).

[12] Z.R. Tian, W. Tong, J.Y. Wang, N.G. Duan, V.V. Krishnan, S.L. Suib Science 276 926 (1997).

[13] Y.F. Shen, S.L. Suib, C.L. O'Young J. Am. Chem. Soc 116 11020 (1994).

[14] H. Cao, S.L. J. Am. Chem. Soc 116 5334 (1994).

[15] A.L. Patterson Phys. Rev. 56, 978 (1939).

[16] M.A. Gabal, S.A. Hameed, A.Y. Obaid Mater. Charact. 71 87–94 (2012).

[17] M. Enhessari, A. Parviz, K. Ozaee, E. Karamali Journal of Experimental Nanoscience 5:161-68 (2010).

[18] M.K. Yadav, A.V. Kothari, V.K. Gupta Dyes Pigments 89 149–154 (2011).

[19] Y. Qu, W. Zhou, H. Fu Chem. Cat. Chem. 6 265–270 (2014).

[20] D.S. Ginley, M.A. J. Appl. Phys 48 2019 (1977).

[21] J. Tauc, R. Grigorovici, A. Vancu Phys. Status Solidi 15 627 (1966).

[22] M. Iwasaki, M. Hara, H. Kawada, H. Tada, S. Ito J. Colloid Interface Sci. 224 202 (2000).

[23] P.N. Kapoor, S. Uma, S. Rodriguez, K.J. Klabunde J. Mol. Catal. A Chem 229 145 (2005).

[24] L. Zhou, S.Y. Zhang, J.C. Cheng, L.D. Zhang, Z. Zeng Mater. Sci. Eng. B 49 117 (1997).

[25] M.W. Li, X.M. Gao, Y.L. Hou, C.Y. Wang J. Nano-and Electronic Phys. 5 3 (2013).

[26] M.S. Sadjadi, K. Zare, S. Khanahmadzadeh, M. Enhessari Mater. Lett. 62 3679-3681 (2008).

[27] Y.J. Lin, Y.H. Chang, W.D. Yang, B.S. Tsai Journal of Non-Crystalline Solids 352 789–794 (2006).

[28] Y. Djaoued, S. Badilescu, P.V. Ashrit, J. Robichaud The Internet Journal of Vibrational Spectroscopy 5 4 (2001).

[29] M. Crisan, M. Zaharescu, A. Jitianu, D. Crisan, M. Preda Journal of Sol-Gel Science and Technology 19 409-412 (2000).

[30] Mizukami Materials Research Bulletin 32 1303-1311 (1997).

[31] D.C. Bradley, R.C. Mehrotra, D.P. Gaur Academic Press New York (1978).

[32] C.M. Phillippi, S.R. Lyon Physical Review B 3 2086-2087 (1971).

[33] S. Musić, M. Gotić, M. Ivanda, S. Popović, A. Turković, R. Trojko, A. Sekulić, K. Furić Materials Science and Engineering B 47 1 33-40 (1997).

[34] S. Liu, Z. R. Tang, Y. Sun, J. C. Colmenares Y. J. Xu Chem. Soc. Rev. 44 5053-5075 (2015).

[35] Y. Zhang, R. Ciriminna, G. Palmisano, Y-J. Xu, M. Pagliaro RSC Adv. 4 18341−18346 (2014).

[36] S. Liu, M-Q. Yang, Z-R. Tang, Y-J. Xu Nanoscale 6 7193−7198 (2014).

[37] L. Yuan, M-Q. Yang, Y-J. Xu J. Mater. Chem. A 2 14401−14412 (2014).

[38] C. Han, M-Q. Yang, N. Zhang, Y-J. Xu J. Mater. Chem. A 2 19156−19166 (2014).

[39] I. Bedjat and P. V. Kamat J. Phys. Chem. 99 9182 (1995).

[40] I. Arslan J. Hazard. Mater. 85 229-241 (2001).

[41] H.B. Hadjltaief, A. Omri, M.B. Zina, P. Da Costa, M.E. Galvez Adv. Mater. Sci. Eng. dx.doi.org/ 10.1155/2015/759853 (2015).

[42] H. Zhu, R. Jiang, Y. Fu, Y. Guan, J. Yao, L. Xiao, G. Zeng Desalination 286 41–48 (2012).

[43] I.A. Alaton, I.A. Balcioglu, D.W. Bahnemann Water Res. 36 1143–1154 (2002).

[44] P. Singla, M. Sharma, O.P. Pande, K. Singh Appl. Phys. A 1–8 (2013).

[45] A. Aleboyeh, H. Aleboyeh, Y. Moussa Dyes Pigm. 57 67–75 (2003).

[46] B. Neppolian, H. Choi, S. Sakthive, B. Arabindoo, V. Murugesan Chemosphere 46 1173–1181 (2002).

[47] A. Weir, P. Westerhoff, L. Fabricius, K. Hristovski, N.V. Goetz Environ. Sci. Technol. 46 2242–2250 (2012).

[48] M. Menzinger, R. Wolfgang Angew. Chem. 6 438–444 (1969).

[49] Y. Guo, S. Yang, X. Zhou, C. Lin, Y. Wang, W. Zhan J. Nanomater. 1–9 (2011).

[50] M. D. Purkayastha, S. Middya, J. Datta, P. P. Ray, B. D. Biswas, M. Sarkar, G. K. Darbha, N. Singh, T. P. Majumder, P. Saha, D. Das Mat. Chem. Phys. 226 362-370 (2019) doi.org / 10.1016 / j.matchemphys. 2019. 01. 049.

[51] M. D. Stamate On the dielectric properties of dc magnetron TiO2 thin films Appl. Surf. Sci. 218 317–322 (2003).

[52] R.S. Joseyphus, E. Viswanathan, C.J. Dhanaraj, J. Joseph Journal of King Saud University Science 24 233-236 (2012) doi. 10.1016/ j.jksus.2011.03.004.